IPPI

Polyolefins Journal, Vol. 6, No. 2 (2019)
DOI: 10.22063/poj.2019.2337.1127

ORIGINAL PAPER

The relationship among changes in microstructure, active sites behavior and properties in the propylene polymerization with a 4th generation Ziegler-Natta catalyst

Shokoufeh Hakim*, Mehdi Nekoomanesh, Ali Shahrokhinia

Department of Polymerization Engineering, Iran Polymer and Petrochemical Institute, P.O. Box: 14965/115, Tehran, Iran

Received: 21 November 2018, Accepted: 22 March 2019

ABSTRACT

Three polypropylene samples (1-3) were synthesized with a 4th generation Ziegler-Natta catalyst in the presence of cyclohexyldimethoxymethylsilane (donor c), dicyclopenthyldimethoxysilane (donor d) and diisopropyldimethoxysilane (donor p), respectively, as external electron donors. The physical properties of the synthesized polypropylenes were determined. For samples 1 to 3, successive self-nucleation and annealing (SSA) and Fourier transform infrared spectroscopy (FT-IR) analyses indicated that the relative content of the fraction with high isotacticity and regularity in conformational structure decreased in contrast with the fraction of low isotacticity and low uniformity in stereo-defect distribution from sample 1 to 3. The results demonstrated that the longer the isotactic sequence length and the less uniform the stereo-defect distribution, the greater the conformational order. Deconvolution of the molecular weight distribution curves indicated that the stability of the active centers increased from samples 1 through 3, but the participation of stereospecific active centers in the polymerization decreased. DMA tests showed that samples 3 and 1 had the highest damping ability and storage modulus, respectively. **Polyolefins J (2019) 6: 139-150**

Keywords: External electron donor; melting point; polypropylene; stereo-defect distribution; Ziegler-Natta catalyst.

INTRODUCTION

Isotactic polypropylene (iPP) has received huge attention due to its unique physical, mechanical and, most importantly, cost-effective properties. [1,2] Currently, the most common catalysts used to synthesize iPP are the fourth generation Ziegler-Natta (Z-N) catalysts, which are based on $MgCl_2$-supported $TiCl_4$ and, dialkyl phthalates, like diisobutyl phthalate, are usually used as internal donor (ID).[3-5] The multiplicity of active centers in Z-N catalysts is well known. Each active center has its own characteristics, including stereo-regularity, transfer and propagation rate constants and activity;[6] so, the final properties and microstructure of the product can be altered via changes in characteristics of the active sites. During the polymerization most of the ID is extracted from the catalyst surface by the alkyl aluminum cocatalyst; therefore, to improve the stereo-regularity of the active sites, an external donor is required. [7-9] The average isotacticity index of iPP can be measured by extraction with boiling n-heptane and ^{13}C NMR analysis.

* Corresponding Author - E-mail: s.hakim@ippi.ac.ir

Crystallinity and the final mechanical properties of polypropylene depend not only on the average isotacticity but also on the stereo-defect distribution, weight average molecular weight (M_w) and molecular weight distribution (MWD).

Several investigations have shown the effects of external electron donors on isotactic sequence length, Mw, MWD, catalyst activity and other properties related to polypropylene. [10-13] We previously showed, using a successive self-nucleation and annealing (SSA) technique, that in the presence of different combinations of donors C and D at a Si/Al molar ratio equal to 0.05, in spite of close average stereo-regularity, the stereo-defect distribution differences among the iPP samples were vast. In addition, the active sites behavior and stereo-specific sequences were altered drastically, resulting in different properties for the final products. [11] Lou et al. studied the effects of two different mono-ethers, namely n-buthyl methyl ether (NBME) and i-buthyl methyl ether (IBME), and diphenyldimethoxysilane (DPDMS) as a silane external donor, on the polypropylene properties synthesized with a 4th generation Z-N catalyst, and on the active sites distribution in the catalyst. They found that composite external donors (mixtures of mono-ethers and the silane external donor) caused more poisoning of a specific active center, enhancement of catalyst activity and isotacticity index and a decrease in melting temperature, compared to systems with only silane as an external donor.[14] Kang et al. investigated the effect of different molar ratios of triethylaluminum (cocatalyst) to dicyclopenthyldimethoxysilane (DCPDMS), as an external donor, on the stereo-defect distribution of isotactic polypropylene by Temperature Rising Elution Fractionation (TREF), SSA and 13C NMR methods. The obtained results indicated that changing the Al/Si molar ratio from 30 to 36, caused the existence of more uniform intra- and intermolecular stereo-defect distribution. [15]

Among the thermal fractionation methods, such as TREF [16] and Crystallization Elution Fractionation (CEF) [17], SSA is more time-saving and is free of solvent, providing useful and quantitative information about the stereo-defect distribution. The stereo-defect distribution influences the movement and crystallization manner of the chains; then, it can be correlated to the conformational behavior of polypropylene. FT-IR can be used as an effective method for investigating the conformational behavior of polypropylene. [18-19] In FT-IR, some absorption bands are sensitive to the physical state and others to the conformation as well as the primary chemical structure of polymers. In the case of iPP, these bands have been categorized into crystal/amorphous, helical and tacticity bands. The IR bands at 940, 1220, 1167, 1303, 1330, 840, 998, 900, 808, 1100 and 973 cm^{-1}, for instance, are related to the helical structure from high to low degree of order or maximum to minimum helix length (helix length is equal to the number of mer units in one regular helix) as listed in the following; [20-22] 940 cm^{-1} ≥14 units, 1220 cm^{-1} =14 units, 1167, 1303 and 1330 cm^{-1} ~13 units, 840 cm^{-1} =12 units, 998 cm^{-1} =10 units, 900 cm^{-1} ~ 8 units, 808 cm^{-1} ~7 units, 1100 cm^{-1} ~ 6 units, 973 cm^{-1} = 5 units. The minimum n values, equal to the number of monomer units in one regular helical segment, are 5, 10, 12 and 14 for the IR bands at 973, 998, 840 and 1220 cm^{-1}, respectively. Obviously, larger n values correlate with higher degrees of regularity.

In this work donor p, as an uncommon external donor, was examined together with donors C and D, individually, in a Si/Al ratio different from that in our previous work. In this investigation, different majorities of stereo-specific sequences, corresponding to short, moderate and long lengths, were synthesized to prove that these external donors, in the individual form and in different Si:Al ratios, altered the microstructure and physical properties of the final products. FT-IR and SSA, as a new approach, were coupled and used to show the relationship between the stereoregularity and regularity in conformational behavior which is critical in determining the crystallinity of the final products. Different behaviors of the active sites were observed, reflecting that they can be poisoned or activated differently by using different kinds of external donors. The quantitative information obtained about the distribution of tacticity, lamellar thickness, conformational behavior and dynamic-mechanical properties proved the possibility of synthesizing samples with broad to narrow distributions of stereo-defects and high to low regularity in conformational behavior by the different kinds of external donors.

EXPERIMENTAL

Materials

Propylene of research grade (purity>99.9%) was supplied by Tabriz Petrochemical Co. (Iran). Nitrogen and hydrogen with purities of 99.99%

were obtained from Roham Gas Co. (Iran) and were passed through columns containing molecular sieves to absorb H_2O, CO_2 and O_2. Triethylaluminum (TEA) and cyclohexyldimethoxymethylsilane (donor c) were purchased from Aldrich Co. and diisopropyldimethoxysilane (donor p) was supplied from Merck Co. (Germany). Dicyclopenthyldimethoxysilane (Donor d) and n-heptane as a diluent (distilled over calcium hydride and stored over 13X and 4A activated molecular sieves and sodium wire) were provided by Arak Petrochemical Co. (Iran). The $MgCl_2/TiCl_4$/DBP (dibuthylphthalate as an internal donor) Ziegler-Natta catalyst was received from the Maroon Petrochemical Co. (Iran) (T_i=2.7% (w/w)).

Propylene polymerization

Polymerization reactions were carried out in a 1L stainless steel Buchi reactor. Before starting the reaction, the temperature of the reactor was raised to 110°C while simultaneously being purged by nitrogen to remove oxygen and humidity. Before beginning the reaction, the reactor temperature was decreased to 40°C while retaining the purge with nitrogen. Then, the reactor was filled with 500ml n-heptane under nitrogen atmosphere, and after that, TEA and the external electron donor diluted in n-heptane were transferred into the reactor under the nitrogen atmosphere. Afterwards, 30 mg of solid catalyst was transferred to the reactor under nitrogen atmosphere (Si/Al and Al/Ti molar ratios were 0.1 and 500, respectively, for all of the external electron donors). As soon as the last injection was done, the propylene valve was opened and a non-isothermal pre-polymerization, in order to reach a better morphology, at 2 bar monomer pressure was begun. Then, hydrogen (120 ml) was injected into the reactor by the Buchi reactor press flow gas controller (bpc 6010) and polymerization at 70°C and 7 bar monomer pressure for 2 hours was continued. After the mentioned polymerization procedure, the reaction was terminated, the vent valve was opened and the unreacted monomer was discharged quickly. The product was dried overnight in an oven at 40°C. The isotacticity index of the polypropylene was determined by the Soxhlet extraction method in boiling n-heptane for 12hr and the weight percentage of the insoluble part was calculated and taken as the isotacticity index (I.I%).

Polymer characterization

Differential scanning calorimetry (DSC)

Crystallization and melting temperatures of the samples were determined by a Pyris 1 DSC, Perkin-Elmer LLC (USA), calibrated with indium metal according to standard procedure. Heating and cooling rates were maintained constant at a standard 10°C/min. The samples were first subjected to a heating ramp to 220°C and kept at this temperature for 5 minutes to remove thermal history. Then, a cooling cycle and second heating ramp were carried out for crystallization and melting analysis, respectively. A value of 209 J/g for the enthalpy of fusion for 100% crystalline polypropylene was used to determine the amount of crystallinity (%) of our samples. [23]

Gel permeation chromatography (GPC)

A PL-210 gel permeation chromatograph Polymer Lab. Ltd. (USA), calibrated [23] according to the universal calibration method with a narrow distribution polystyrene standard using 1,2,4-trichlorobenzene as solvent at 140°C, was used to determine the molecular weight and molecular weight distribution of the samples. The samples were dissolved in the solvent at 135°C for 6 hr with stirring, and then the tests were done at 130°C.

Successive self-nucleation and annealing (SSA) fractionation

SSA fractionation was carried out according to the following steps: a) removing the thermal history by heating the samples to 220°C and keeping them at this temperature for 5 min, b) cooling the samples with the rate of 20°C/min to 30°C and holding at this temperature for 2 min, c) heating the samples with the rate of 20°C/min from 30°C to a T_s (a denoted partial melting temperature), d) holding the samples at the mentioned T_s for 15 min, e) subjecting the samples to a cooling cycle from T_s to 30°C with the rate of 20°C/min (reflection of thermal treatment on crystallization of samples), f) repetition of steps 3 to 5 for successively lower T_s, varied from 167°C to 139°C with 4˚C intervals, according to reference;[24] at the end, the samples were heated with the rate of 10°C/min from 30°C to 200°C and the results were recorded.

Fourier transform infrared spectroscopy

Molding the samples into thin films at 220°C and

pressure of 10 MPa was done by a platen press. Then, to obtain the same thermal history, all were cooled down with the same procedure by running cold water through the platens at the same rate for all samples. The spectra were recorded at 26°C using a Bruker Vertex/80v FT-IR spectrometer (Germany) with a resolution of 4 cm^{-1} and 16 scans. The range of scanned wave numbers was 400-4000 cm^{-1}.

Dynamic – mechanical analysis (DMA)

The dynamic-mechanical analysis of rectangular samples with known dimensions (length~18.5mm; width~10mm; thickness~4mm) was carried out with a 2000-Tritec DMA instrument Triton Technology Ltd. (England). A single cantilever clamp at a clamping force of 120N, constant frequency of 10Hz and amplitude of 20mm was used with sampling intervals of 2s/pt in a temperature range between minus 30°C and 130°C and a heating rate of 3°C/ min.

RESULTS AND DISCUSSION

Characteristics of samples

The general information about the samples is listed in Table 1. The isotactitcity indices of samples 2 and 3 were approximately the same but the slightly better effect of donor c in sample 1 could be related to its higher ability in the poisoning of aspecific active centers and the activation effect of isospecifc active centers during the polymerization when the Si/Al molar ratio was 0.1. The activity of the catalyst for sample 1 was the highest. It has been reported that by the introduction of external donors, a tangible fraction of the active centers are deactivated and eliminated.[2] Then, the only logic for the different activity in the presence of different external donors can be related to the variety of active site elimination trend, shown by different external donors. The noticeable decrease in melting temperature from sample 1 to 3 corresponds to the formation of lower lamellar thicknesses for the same cooling rates (according to Thomson-Gibbs in Eq. 1) that could be a sign for the existence of different distributions of stereo-defects and crystallizability in the synthesized samples.

$$T_m = T_m^0 \left(1 - \frac{2\delta}{\Delta H_0 L}\right) \quad (1)$$

In Eq. 1, T_m^0 = 460 K [25] (equilibrium melting temperature), ΔH_o = 184×106 J/m^3 (equilibrium melting enthalpy per unit crystalline volume), δ = 0.0496 J/m^2 (surface energy) and L is the lamellar thickness. Crystallinity (%) and crystallization peak temperature decreased from sample 1 to 3. Higher stereo-regularity and lower molecular weight of polymers, with fewer entanglements inhibiting crystallization, led to higher degrees of crystallinity (%). Therefore, the lower amount of crystalline phase in sample 3 can be explained. The presence of donor p in the polymerization system, which resulted in a decrease of transfer reaction rate constants (K_t), might have stabilized the active centers in this polymerization system. According to Scheme 1, in the presence of donor p, the amount of time which is spent in the isotactic side can be enhanced. The formation of different kinds of active centers is shown in Scheme 1 in which the AlR_3, ED and the oval are the indications of cocatalyst, external donor and the vacant site, respectively. The free sites (without external donors and with two vacant sites) always react more easily with hydrogen; thus, the presence of external donor like donor p, the occupation of one vacant site in the active site and shifting to isotactic side decrease the frequency of hydrogen transfer reactions. Reduction in hydrogen transfer

Table 1. Some characteristics of the synthesized i-PPs.

Code	ED[(a)]	I.I(%)[(b)]	M_w [(d)] (g/mol)	X_c [(c)] (%)	Melting temperature (°C)	PDI[(d)]	Crystallization temperature (°C)	Activity [(f)] (Kg PP/gTi.hr)	T_g [(e)] (°C)
1	C	95.2	190000	49	162	3.9	112	52	7
2	D	94.2	172000	49	159	4.3	110	41	6
3	P	94.1	717000	46	159	5.6	107	48	8

[(a)] The name of external electron donors used in the polymerizations.
[(b)] Isotacticity index (%) expressed as percentage of boiling *n*- heptane insoluble fraction.
[(c)] Crystallinity (%) determined by DSC tests from melting enthalpy.
[(d)] Polydispersity index and molecular weight determined by GPC tests.
[(e)] Glass transition temperatures determined with DMTA tests.
[(f)] The average of activity for two batches (difference of activity for the two batches was maximum 5%).

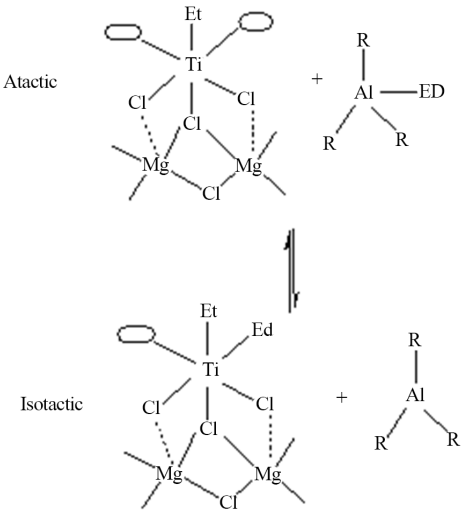

Scheme 1. Equilibrium between isotactic and atactic active sites.

reaction rate constant and less fluctuation in the active site situations between the two sides in Scheme 1 caused the higher molecular weight in sample 3. In addition, the insertion of more stereo-defects into the chain due to less transfer reaction frequency with hydrogen can be another explanation for the slightly lower average stereo – regularity in sample 3.

Successive self-nucleation and annealing analysis

For the same crystallization conditions, the stereo-defects distribution and average isotacticity index of the iPPs have the main role in determining the thickness of the formed lamellae, their thickness distribution and the final properties of the samples, which can be well investigated by the successive self-nucleation and annealing (SSA) thermal fractionation technique. During SSA, self-nucleation and annealing are applied to a polymer step by step to fractionate the molecules during crystallization and to anneal unmolten crystals at each stage. [16,26] Figure 1 shows the SSA final melting curves of samples 1-3. The shapes of the curves for the three samples are different which can be correlated to their differences in stereo-defects and lamellar thickness distributions. In Figure 2, the related SSA curves are fitted into 8 individual Gaussian-shaped peaks using Peakfit 4.12 software. For comparison, these peaks were divided into 3 main groups: I, the peak located in the highest temperature region (>175°C); II, the peak located in the middle temperature region (168-175°C); and III, the peaks located in the lowest temperature region (<168°C). According to equation 1, peak 1 is attributed to the melting of the thickest lamellae and the highest isotactic sequence length, peak 2 is related to the medium lamellar thickness and isotactic sequence length and peaks 3 corresponds to the lowest lamellar thicknesses and the shortest isotactic sequence lengths.

Analysis of the SSA results of the iPP samples

In order to have qualitative and quantitative information from the SSA results, the relative area percentages (i.e., the integral area percentages under the various peaks in the final SSA melting curves) of the three mentioned groups were calculated. The results are given in Table 2. As indicated for sample 1, compared with the other samples, the relative content of peak 1 was the highest and the relative content of peaks 3 was the least. The relative content of peaks 3 increased from sample 1 to 3 (45 to 53%); meanwhile, the relative content of peak 1 decreased drastically from sample 1 to 2 (15 to 0%) and then increased slightly from sample 2 to 3 (0 to 5%). In the case of peak 2, an increase from sample 1 to 2 (40 to 49%) and then a decrease from sample 2 to 3 (49 to 42%) can be seen.

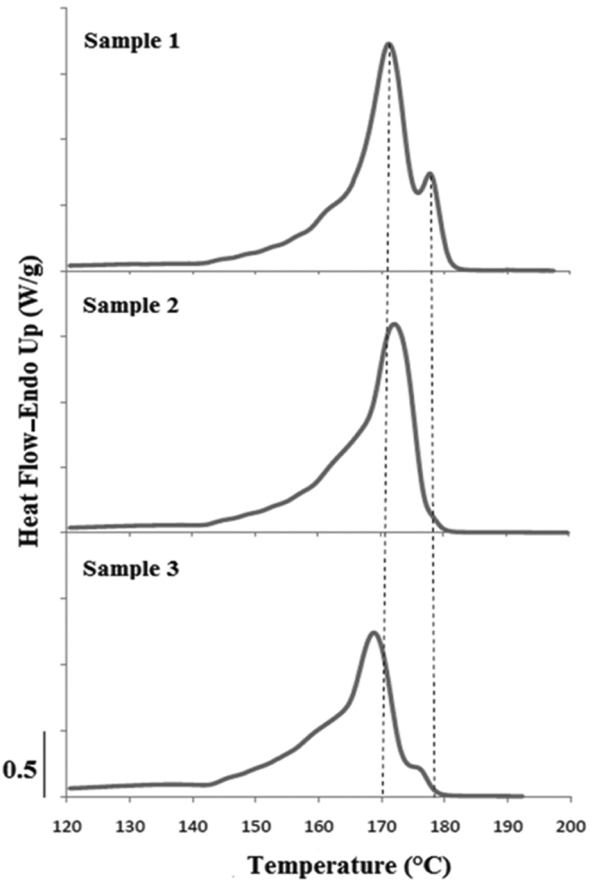

Figure 1. Final melting curves of three samples. The dashed lines are indications for the difference in the location of peaks1 and 2

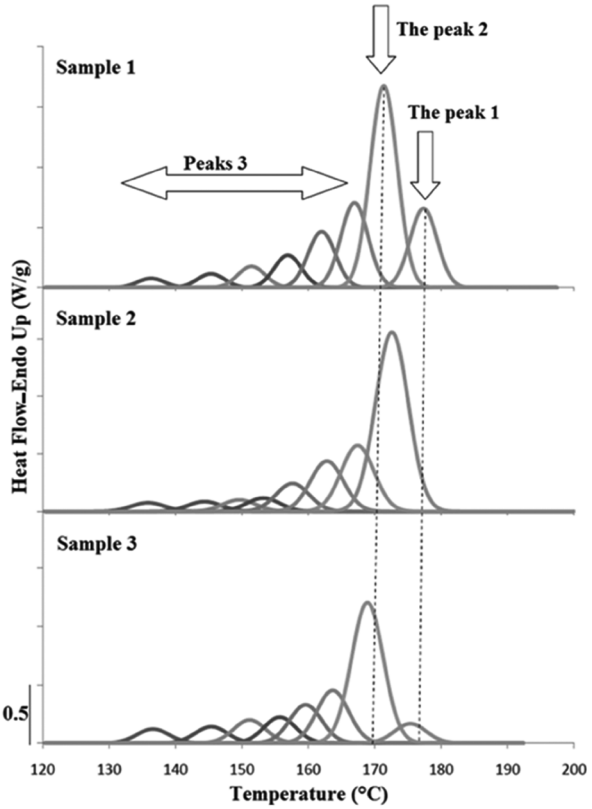

Figure 2. Related fitted peaks for the SSA final melting curves using Peakfit 4.12 software. Peak 1: The peak located in the highest temperature region (>175°C), Peak 2: The peak located in the second temperature region (168-175°C),Peaks 3: The peaks located in the lowest temperature region (< 168°C).The dashed lines are indications for the difference in the location of peaks 1 and 2.

For further analysis, the statistical parameters describing the lamellar thickness, i.e., the arithmetic average lamellar thickness (L_n), weighted average lamellar thickness (L_w), broadness index (I), arithmetic average isotactic sequence length in one fold for the lamellar (ISL_n)(propylene units) and weighted average isotactic sequence length in one fold for the lamellar (ISL_w) (propylene units) were calculated using equations 2 to 5. The results are given in Table 3.

Table 2. Relative content of the peaks (%) in each of the three areas for the three samples.

Sample code	Donor code	Peak (%) (1)	Peak (%) (2)	Peaks (%) (3)
1	C	15	40	45
2	D	0	49	51
3	P	5	42	53

Peak 1: The peak located in the highest temperature region (>175°C)

Peak 2: The peak located in the second temperature region (168-175°C)

Peaks 3: The peaks located in the lowest temperature region (< 168°C)

$$L_n = \frac{n_1L_1 + n_2L_2 + ... + n_jL_j}{n_1 + n_2 + ... + n_j} = \sum f_i L_i \quad (2)$$

$$L_w = \frac{n_1L_1^2 + n_2L_2^2 + ... + n_jL_j^2}{n_1L_1 + n_2L_2 + ... + n_jL_j} = \sum f_i L_i^2 \quad (3)$$

$$I = \frac{L_w}{L_n} \quad (4)$$

$$ISL = \frac{3L}{L_{helix}} \quad (5)$$

In the equations, ni is the normalized partial area of the fractions in the final SSA curves and Li is the lamellar thickness for each fraction. In equation 5, L is the lamellar thickness and L_{helix} is the length of one crystal unit cell along the chain direction. For the unit cell of the monoclinic α form, the c axis, corresponding to the chain direction, is 0.65 nm. In this direction, one unit cell contains 3 monomers, L_{helix} = c = 0.65 nm [27] (L/3 = the c axis projected length of one mer). It is seen from Table 3 that L_n, L_w, ISL_n and ISL_w decrease from sample 1 to 3, which is attributed to the existence of longer isotactic sequence lengths in one fold and thicker lamellae in the presence of donor c. In other words, the greatest chance for higher frequency of stereo-regular monomer insertion to result in longer isotactic chain length in active centers was obtained in the presence of donor c and the high frequency of stereo-irregular monomer insertion, resulting in lower isotactic chain length, can be seen in the presence of donor p. Moreover, the broadness index (I) for donor c was the highest which could be explained by more heterogeneity of active centers in frequency of stereo-regular monomer insertion and indicates that the thickness distribution of the lamellae became broader in the presence of donor c. The broadness indices for samples 2 and 3, which are due to the presence of donors D and P, respectively, are less than that in sample 1, and very close.

The SSA results clearly showed that the distribution of stereo-defects of the samples was different. The location of each peak in Figure 2 was used for comparison of the isotactic sequence lengths in one fold among the three samples. As can be seen, peak 1 is located in the highest temperature region in sample 1, which indicates the thickest lamella with the longest isotactic sequence lengths in one fold, which are the result of the presence of donor c. Peak 2, related to the moderate lamella thicknesses with the moderate isotactic sequence lengths in one fold, is located in the

highest temperature region in the presence of donor d (sample 2). In the group related to the thinnest lamella thicknesses with the shortest isotactic sequence lengths in one fold (peaks 3), the active centers produced the longest isotactic chain length (the highest T_m for the highest T_{peak}) in sample 2. This could be another explanation for the higher melting temperature of sample 2, compared with that in sample 3 and a sign for a greater tendency of active centers in formation of longer isotactic sequence length in the moderate and low isotactic chain length groups (peaks 2 and peaks 3 respectively) in the presence of donor d. Thus, by using different kinds of individual external donors and in different Si:Al molar ratios, a different majority of stereo-specific sequences and the stereo defect distribution, compared to those in our previous work, were obtained[11]. In that case, for the Si:Al molar ratio of 0.2 and in the presence of donors c and d individually the majority of chains had short isotactic sequence length in one fold (83 and 84% for peaks 3 respectively) and shorter lamellae thicknesses (11.2 and 11.8 nm respectively) compared to those for the Si:Al molar ratio of 0.1.

Fourier transform infrared spectroscopy

From a new point of view, compared to our former article, [11] in which only the configuration behavior of the chains was studied, here the relationship between the stereo-regularity and regularity in conformational behavior was investigated. The FT-IR spectra of the samples shown in Figure 3 were used to clarify the conformational structure of the samples and to determine its relationship with the stereo-defect distribution. Because each IR band has its own intensity coefficient, it was required to identify the intensities of the regular helical conformation bands. Hence, in the present study, the variation in relative intensities of A998, A840 ,and A1220 (973 cm^{-1} as internal references), indicating relative absorbance intensities of helical sequences with 10, 12 and 14 monomer units, respectively [20], was used to compare the regularity in helical conformation. To obtain better comprehension, the relative intensities of sample 1 were taken as references. The results are shown in Figure 4. The relative intensities of A998, A840 and A1220, were the highest for sample 1. From sample 1 to 3, A998 decreased slightly but in the case of A840 and A1220, from sample 1 to 3, the mentioned relative intensities first decreased and then remained constant. The stereo-defect distribution can influence the folding manner of the chains and repeating unit movement. The studied helical length or conformational order degree which is attributed to the isotactic sequence length and stereo-defect distribution in the chains, was the highest for sample 1(especially those sequence lengths which are the stimulator and borderline in the crystallization occurrence). Therefore, as the isotactic sequence length becomes longer, the stereo-defect distribution becomes less uniform and lower molecular weights are obtained, and less restriction on molecular ordering and more conformational ordering are more likely to result. From the view point of the crystallization process, it is known that if the persistence length of 31 helical sequences exceeds 12 monomer units (shown by the regularity bands at 840 cm^{-1} and the bands related to the longer helical length) the melt state of polypropylene will be unstable at temperature below the T_c, parallel ordering will begin and then crystallization will occur. [22] As can be observed from Figure 4, the normalized relative intensities could be a sign for the existence of a higher majority of longer helical lengths in sample 1 than in the other samples (more than 10 mer units for the same thermal history). Therefore, it is logical to say that sample 1 has the greatest potential for crystallization. Thus, the results in this section are in good coincidence with the results obtained from the DSC and SSA tests.

Investigation of the characteristics of the active centers

The MWD curve of sample 1, deconvoluted into the four most-probable Flory components by MATLAB R2010a software, is shown in Figure 5. Since the Ziegler-Natta catalysis has multiple active centers and broad PDI, it is mandatory to divide the MWD (mo-

Table 3. Lamellar thickness parameters, number average and weight average isotactic sequence length.

Sample code	Donor code	L_n (nm)	L_w (nm)	I	ISL_n (PP unit)	ISL_w (PP unit)
1	C	14.5	16.9	1.16	66.9	77.9
2	D	13.4	14.7	1.10	61.8	68.1
3	P	11.4	12.7	1.11	52.7	58.7

(ISL_n and ISL_w) calculated from SSA melting curve for three samples.

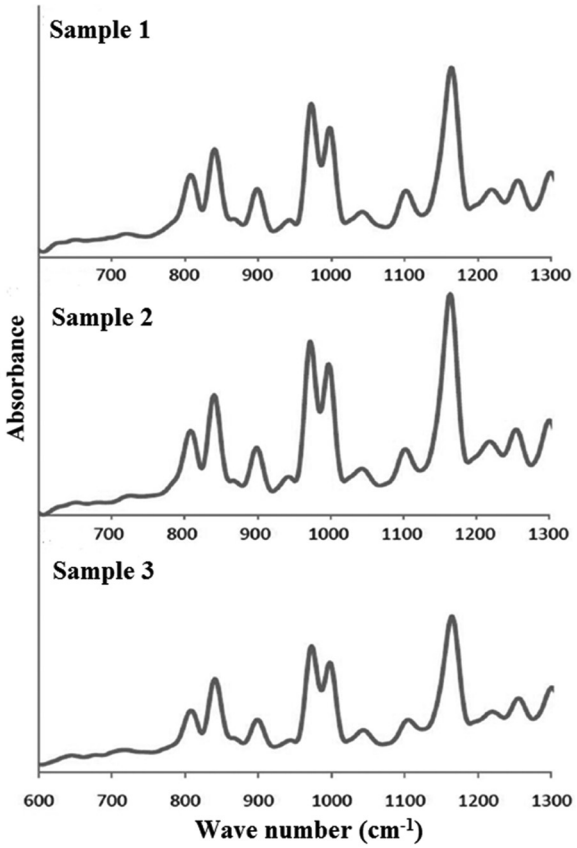

Figure 3. FT-IR Spectra of Samples 1-3.

lecular weight distribution curve) and active centers into their Flory components, possessing a narrow PDI. Each Flory component represents a certain type of catalyst active center that results in polymer molecules with intrinsic weight and number average molecular weights (M_{wi} and M_{ni}), PDI equal to 2 and consists of a certain mass fraction of the whole polymer (m_j). So, the MWD of a polymer (w (log M_w)), made with a Z-N catalyst, can be described by the summation of the different Flory components according to Equation 6 [28,29]. Here, m_j is the weight fraction of the polymer made on one of the four sites j, τ is the inverse of the overall M_n and τ_j is the inverse of M_n produced by the active site j.

$$w(\log M_w) = 2.3026(M_W)^2 \tau^2 \sum_{i=1}^{4} m_j \tau_j^2 \exp(-M_W \tau_j) \quad (6)$$

The mass fractions and number average molecular weights of the polymer chains produced in each active center are shown in Figures 6 and 7, respectively. The fraction percentage of active sites A and B increased from samples 1 to 3 but, on the other hand, the fraction percentage of active sites C and D decreased from samples 1 to 3. It has been proved that the molecular weight of various fractions of a polypropylene, synthesized by a Z-N catalyst, is directly related to their isotacticty [30] (the isotacticity increases with the increase in the chain length and vice versa for different fractions). Therefore, the polypropylene chains which were produced by active sites C and D, having higher Mw, had higher tacticity than those produced by active sites A and B. It can be concluded that donor p, used for synthesizing sample 3, resulted in producing a higher fraction percentage of sites A and B, and thus had the weaker ability for selective poisoning of non-stereo specific active centers. On the other hand, donor c had the highest ability for selective poisoning of non-stereo-specific active sites, resulting in having the highest activity of sites C and D and the least activity of sites A and B.

Different participations of active centers in a polymerization system can cause different stereo-defect distributions among the polymer chains. So, it is logical to conclude that the higher activity of active sites A and B could be a reason for the majority of thinner lamellae in sample 3 via the majority of shorter isotactic sequence lengths and, in the opposite point, more participation of active sites C and D for synthesizing sample 1 is the main proof for the existence of thicker lamellae, resulting from the higher percentages of long isotactic sequence lengths. It is shown in Figure 7 that the number average molecular weight of each active site from samples 1 to 3 first decreased slightly for sample 2 and then increased sharply. So, it can be deduced that the active centers in the presence of donors P and D had the most and least stability or the least and most frequency of transfer reaction

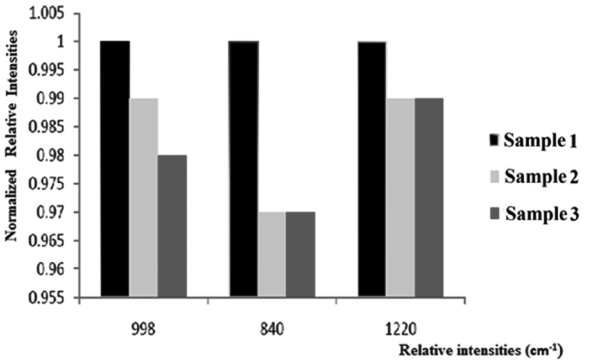

Figure 4. Relative intensities of different regularity bands of the three samples. (The intensities of each of the bands of sample 1 were used as references).

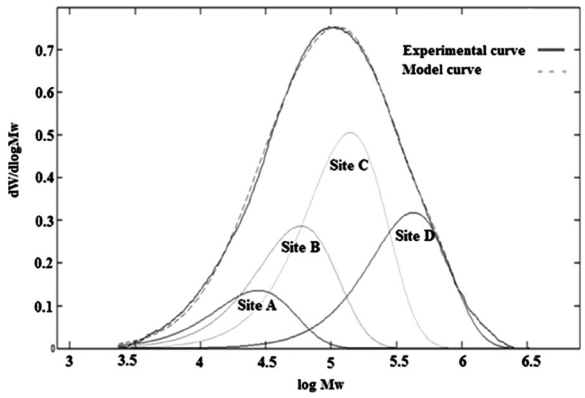

Figure 5. Deconvoluted MWD curve into its Flory components for sample 1.

occurrence, respectively. In contrast with our former article [11], instead of moderate isospecific active centers, the present non-stereo and highly specific active ones were influenced by individual external donors for the used Si:Al ratio which drastically changed the arrangement of monomers in the polymer chains.

Dynamic-mechanical properties

The curves for storage modulus and tan delta versus temperature are shown in Figures 8 and 9, respectively. In the case of the storage modulus (Figure 8), at temperatures below the rubbery region and glass transition temperature, the higher molecular weight of sample 3, which caused more entanglements among the chains, was the determining factor for the observed difference. Above the temperature of the glassy region, in the rubber region, the greater crystallinity(%) of sample 1 and the existence of thicker lamellae in it, compared to sample 3, was the determining factor for its higher storage modulus due to the increase in chain

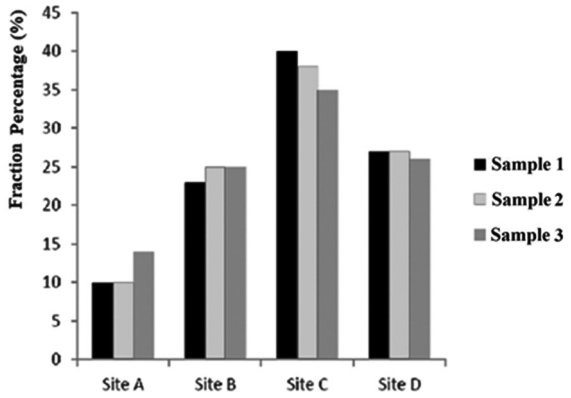

Figure 6. Fraction of each Flory component in samples 1 to 3.

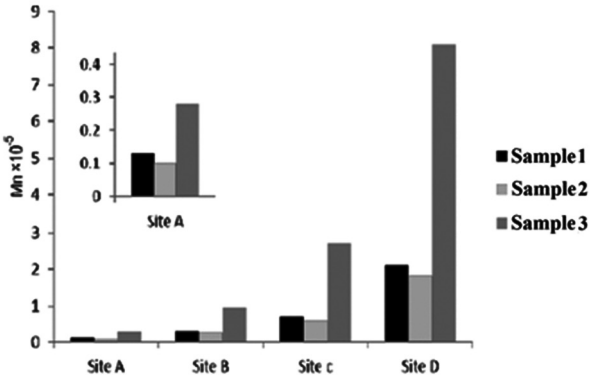

Figure 7. Related number average molecular weight of each Flory component in samples 1 to 3.

mobility restriction. Tan delta curves indicate the ability of a material to lose energy, being related to its damping ability. Samples 3 and 1 had the highest and lowest tan delta values, respectively, over the entire temperature region and particularly above T_g. This difference can be explained by the slightly different crystallinity (%), lamella thickness and the existence of different amounts of short chains. Slightly less crystallinity (%) and thinner lamella thickness, resulting in more ability of chains movement, can be influential for increasing the damping ability of the samples. In addition, higher percentages of short chains, playing a major role as a lubricant, attributed to the higher activity of non-stereo specific active sites and broader MWD, can be responsible for enhancing the damping ability of a polymer. Thus, because of the lower crystallinity (%) of sample 3, the existence of thinner lamellae (shown in Tables 1 and 3) and higher activity

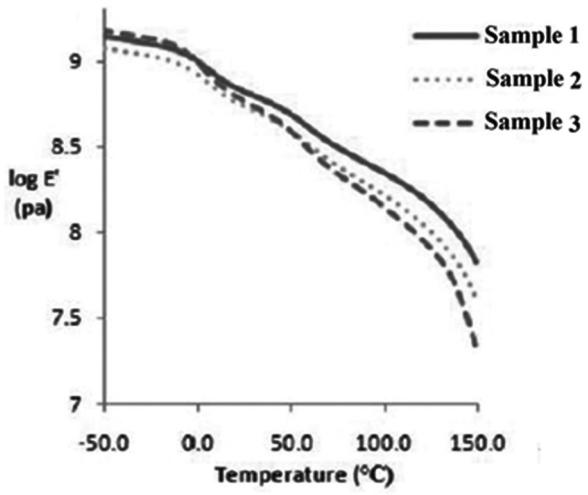

Figure 8. Variation of storage modulus versus temperature in samples 1 to 3.

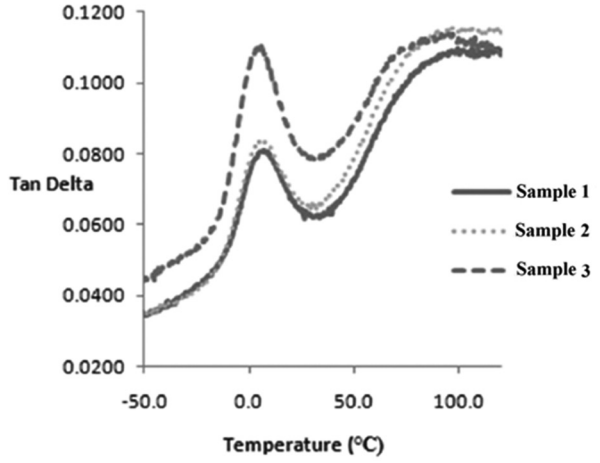

Figure 9. Variation of tan delta versus temperature in samples 1 to 3.

of site A in it (Figure 6), which are reversed for sample 1, the highest damping ability of sample 3 and the lowest one for sample 1 are logical. It is seen in Table 1 that, among the three samples, T_g of sample 3 was the highest (as it has the highest molecular weight, there are more entanglements in the amorphous phase and thus more restrictions of the chains). Consequently, the above-mentioned results of the DMA tests reflected that individual external donors at a Si:Al ratio equal to 0.1 can act as a factor to diversify the dynamic-mechanical properties of the final products.

CONCLUSION

In this study, three polypropylene samples (1, 2 and 3) were synthesized in the presence of three different external electron donors c, d and p, while other reaction conditions were kept constant. For samples 1 to 3, the Mw, MWD and glass transition temperature increased in the order of sample1, sample 2 and sample 3, but the isotacticity index, crystallinity (%), melting temperature and crystallization temperature increased in reverse order. The activities of the catalyst in the presence of donors c and d were the highest and lowest, respectively. The SSA and FT-IR results coupled with each other showed that longer isotactic sequence length, less uniform stereo-defect distribution and lower molecular weight, resulting in less restriction on ordering of the chains, created more conformational order. The SSA results also showed that even though the overall isotacticity of the samples are close, the stereo-defect distribution of the three samples were greatly different. Thus, in the presence of different external electron donors, different stereo-defect distributions and isotactic sequence length majorities can be achieved. The FT-IR results also indicated that among the three samples, the degree of conformational order of sample 1 was the highest and the stereo-defect distribution played the main role in determining the degree of conformational order of the iPPs. According to deconvolution of the MWD curves of the three samples, donor c had the most ability for poisoning aspecific active centers (sites A and B) and activation of isospecific active centers (sites C and D). On the other hand, the active centers in the presence of donor p had the most stability (reduction of transfer reaction rate and/or increase in propagation rate). It was obvious from the DMA results that the stereo-defect distribution, crystallinity (%) and active site behavior had significant effects on the dynamic-mechanical properties of the iPPs.

REFERENCES

1. Genis AV (2015) Analysis of the global and Russian markets of polypropylene and of its main consumption area. Russ J Electrochem 87: 2137-2150
2. Shen X, Fu Z, Hu J, Wang Q, Fan Z (2013) Mechanism of propylene polymerization with Mg-Cl_2 supported Ziegler-Natta catalysts based on counting of active centers: The role of external electron donor. J Phys Chem C 117: 15174-15182
3. Piryanshu B, Sukhdeep K, (2011) Synthesis of polypropylene with varied microstructure and molecular weights characteristics using supported titanium supported catalyst system. J Polym Res 18: 235-239
4. Zohouri G, Kasaeian A, Angagi M, Jamjah R, Mousavian A, Emami M, Ahmadjo S (2005) Polymerization of propylene using $MgCl_2$ (ethoxide type)/$TiCl_4$/diether heterogenous Ziegler-Natta catalyst. Polym Int 54: 882-885
5. Zohouri G, Azimfar F, Jamjah R, Ahmadjo S, (2002) Polymerization of propylene using the high activity Ziegler_Natta catalyst system SiO_2/$MgCl_2$ (Ethoxide type) /$TiCl_4$/Di-n-buthyl phthalate/Triethylaluminium/Dimethoxy Methyl Cyclohexyl Silane. J Appl Polym Sci 89: 1177-1181
6. Maddipati SV, Delgass WN, Caruthers JM, (2011)

Determination of the catalytic sites for Ziegler Natta homo-polymerization from GPC data. Macromol Theory Simul 20: 31-45
7. Kim SY, Hiraoka Y, Taniike T, Terano M, (2009) External donor induced direct contact effects on $Mg(OC_2H_5)_2$ – Based Z-N catalysts for propylene polymerization. Macromol Symp 285: 115-120
8. Matsouka H, Liu B, Nakatani H, Nishiyama I, Terano M (2002) Active sites deterioration of $MgCl_2$ supported catalyst induced by the electron donor extraction by alkylaluminum. Polym Int 51: 781-784
9. Potapov A.G, Bukatov G.D, Zakharov V.A (2010) DRIFTS study of the interaction of the Internal donor in $TiCl_4$ di-n-butyl phthalate/$MgCl_2$ catalysts with $AlEt_3$ cocatalyst. J. Mol. Catal A: Chem 316: 95-99.
10. Piryanshu B, Sukhdeep K (2011) Synthesis of polypropylene with varied microstructure and molecular weights characteristics using supported titanium supported catalyst system. J Polym Res 18: 235-239
11. Hakim S, Nekoomanesh M, Shahrokhinia A (2015) The effect of mixed and individual silane external donors on the stereo-defect distribution, active sites and properties of polypropylene synthesized with fourth generation Ziegler-Natta catalyst. Polym Sci-A 25: 573-580
12. Vestberg T, Denifl P, Parkinson M (2010) Effects of external donors and hydrogen concentration on oligomer formation and chain end distribution in propylene polymerization with Z-N catalysts. J Polym Sci Pol Chem 48: 351-358
13. Chadwick J, Morini G, Balbontin G (2001) Effects of Internal and External donors on regio and stereoselectivity of active species in $MgCl_2$ supported catalysts for propene polymerization. Macromol Chem Phys 202: 1995-2002
14. Lou J, Tu S, Fan Z, (2010) Polypropylene chain structure regulation by alkoxy silane and ether type external donors in $TiCl_4$/DIBP/$MgCl_2$-$AlEt_3$ Ziegler-Natta catalyst. Iran Polym J 19: 927-936
15. Kang J, Feng Y, Tong W, Huilin L, Ya C, Ming X (2012) Polymerization control and fast characterization of the stereo-defect distribution of heterogeneous Ziegler-Natta isotactic polypropylene. Eur Polym J 48: 425-434
16. Xu J, Feng L, Yang S, Yang Y, Kong X (1998) Temperature rising elution fractionation of polypropylene produced by heterogeneous Ziegler-Natta catalysts. Eur Polym J 34: 431-434
17. Monrabal B, Sancho-Tello J, Mayo N, Romero L, (2007) Crystallization elution fractionation. A new separation process for polyolefin resins. Macromol Symp 257: 71-79
18. Zhao J, Peng Z, Zhang J, Li J (2011) In situ FT-IR spectroscopy study on the conformational changes of quenched isotactic polypropylene during stepwise heating. Polym Bull 67: 1649-1659
19. Li B, Li L, Zhao L, Yuan W (2008) In-situ FT-IR spectroscopic study on the conformational changes of isotactic polypropylene in the presence of supercritical CO_2. Eur Polym J 44: 2619-2624
20. Zhu X, Yan D, Yao H, Zhu P (2000) In situ FT-IR spectroscopic study of the regularity bands and partial-order melts of isotactic poly(propylene). Macromol Rapid Commun 21: 354-357
21. Kang J, Yang F, Wu T, Li H, Liu D, Cao Y, Xiang M (2012) Investigation of the stereo-defect distribution and conformational behavior of isotactic polypropylene polymerized with different Ziegler-Natta catalysts. J Appl Polym Sci 125: 3076-3083
22. Zhu X, Yan D, Fang Y (2001) In situ FT-IR spectroscopic study of the conformational change of isotactic polypropylene during the crystallization process. J Phys Chem B 105: 12461-12463
23. Brandrup J (1989) Polymer Handbook. Wiely, 90-95
24. Fillon B, Wittmann J.C, Lotz B, Thierry A (1993) Self nucleation and enhanced nucleation of polymers. Definition of a convenient calorimetric efficiency scale and evaluation of nucleating additives in isotactic polypropylene. J Polym Sci Pol Phys 31: 1383-1393
25. Wlochowitcz A, Eder M (1984) Distribution of lamella thicknesses in isothermally crystallized polypropylene by differential scaning calorimetry. Polymer 25: 1268-1270
26. Garoff T, Virkkunene V, Jaaskelainen P, Vestberg T (2004) qualitative model for polymerization of propylene with a Z-N catalyst. Eur Polym J 39: 1679-1685
27. Paolini Y, Ronca G, Feijoo J, Silva E, Ramirez J, Muller A (2001) Application of SSA calorimetric technique to characterize an XLPE insulator aged under multiple stresses. Macromol Chem Phys 202: 1539-1547

28. Fan Z, Feng L, Yang S (1996) Distribution of active centers on $TiCl_4/MgCl_2$ catalyst for olefin polymerization. J Polym Sci Pol Chem 34: 3329-3335
29. Kissin YV, (1995) Molecular weight distribution of linear polymers: Detailed analysis from GPC data. J Polym Sci Pol Chem 33: 227-237
30. Kioka M, Makio H, Mizuno A, Kashiwa N (1994) Tacticity distribution of polypropylene prepared by $MgCl_2$- supported titanium catalyst. Polymer 35: 580-583